Graphs List

please go to ↓ directory.
/arthur/users/ta/MODELS/TRAIN/

"0.15" means "constrained model"

Directory	***File Name***
Penetration Depth	
□ /depth/	= Fig. A3a.eps
□/depth/ PREDICTIONS/	= Fig. 1a~3b.eps
□/depth0.15/	= Fig. A3b.eps
Area	
□/area/	= Fig. A4a.eps
□/area/PREDICTIONS/	= Fig. 4a~6b.eps
□/area0.15/	= Fig. A4b.eps
Top-width	
□/topwidth/	= Fig. A5a.eps
□ /topwidth/PREDICTIONS/	= Fig. 7a~9b.eps
□/topwidth0.15/	= Fig. A5b.eps
Bottom-width	
□/bottomwidth/	= Fig. A6a.eps
□ /bottomwidth/PREDICTIONS/	= Fig. 10a~12b.eps
□/bottomwidth/	= Fig. A6b.eps
Height	
□/height/	=Fig. A7a.eps
□/height/PREDICTIONS/	= Fig. 13a~15b.eps
□/height0.15/	= Fig. A7b.eps

Table. 1, Fig. A1, Fig. A2 and paper are in floppy disc.

use "SURFER" in windows

Takashi Shimada

Modelling of Plasma-Augmented-Laser-Welding

TAKASHI SHIMADA, YOSHIYUKI SAITO[1] and H. K. D. H. BHADESHIA[2]

Undergraduate student, Department of Materials Science and Engineering, Waseda University, 3-4-1 Okubo, Shinjuku-ku,Tokyo 169-8555 Japan.

1) Department of Materials Science and Engineering, Waseda University, 3-4-1 Okubo, Shinjuku-ku, Tokyo 169-8555 Japan.

2) Department of Materials Science and Metallurgy, University of Cambridge, Pembroke Street, Cambridge CB2 3QZ, UK.

Abstract

This work deals with a welding process involving two separate heat sources, the plasma-augmented-laser-welding process. Experimental data are available on the variation in weld pool characteristics as a function of the welding parameters. These data were analysed in two ways. In the first method, the data were used for training neural network within a Bayesian framework, permitting the model to find its own perceived level of noise in the output. This led to results in which the mean trends were meaningless by assigning large uncertainties (error bars). An analysis of the experimental data showed that they are extremely noisy. It was therefore decided to constrain the neural network to avoid training to a noise level better than 0.15. This resulted in physically significant trends. It is concluded that the latter model is a better representation of noise and sparse data.

1. Introduction to process

Neural networks are powerful tools designed to implement non-linear regression analysis using a very flexible mathematical function. It is then possible to recognize patterns and draw conclusions from complex, noisy and often irrelevant information [1]. Therefore it has recently been used for a wide variety of materials science application. For example, the plasma-augmented-laser-welding process [2~4] is new and it would be very helpful to have a model which estimates the shape of the weld pool as a function of process variables. It is with this in mind that Vitek et al. developed a neural network model for the weld pool geometrical-parameters as a function of the arc current, laser power and welding speed. However, the model they used did not include a calculation of the uncertainty of fitting, so it was difficult for them to assess the value of extrapolation.

One aim of the present work was to repeat the analysis using a neural network technique due to MacKay. This particular method is within a Bayesian framework and in addition to an estimate of the perceived level of noise in the output, it also gives a powerful indication of the uncertainty of fitting. Furthermore, the magnitude of the latter error bar is presented, as a function of the position in the input space, i.e., there is a warning of the scarcity of knowledge when calculations are done using inputs where the model is uncertain.

2. Method of Neural Network

The input data x_j are multiplied by weights w_j and the sum of these products form the argument of a hyperbolic tangent:

$$h=\tanh\left(\sum_i w_j^{(1)} x_j+\theta\right) \text{ with } y=w^{(2)}h+\theta^{(2)}$$

where $w^{(2)}$ is a weight and $\theta^{(2)}$ is an another constant.
The strength of the hyperbolic-tangent transfer function is determined by the weight w_j. The output y is therefore a non-linear function of x_j, the function usually chosen being the hyperbolic-tangent because of its flexibility.
Altering the weights can vary the exact shape of the hyperbolic-tangent. The control of over-fitting is designed elsewhere [1].

3. Model Characteristics

In order to preserve clarity, the detailed characteristics of the neural network models, for example, the variety of errors and committee structures, are presented separately in the appendix. However, some important features are described here.
It was realized at an early stage in the analysis, that the experimental data are extremely noisy. This is clearly illustrated in Fig. A1 which is a contour plot of the ratio of power to speed (a measure of the laser energy input per unit length) versus the ratio of the current to speed (a measure of the arc energy input per unit length). The contours represent the penetration depth in dimensions of mm. This plot of the experimental data shows clearly that the same values of the input parameters lead to quite different values of the output which is the penetration depth.
This indicates that the experiments are not well controlled. There are two options in modeling such extremely noisy data. Firstly, the neural network in the Bayesian network can be used in an *unconstrained* form, allowing it to reach the correct *average* value of the perceived level of noise σ_v in the normalised value of the penetration depth. Any poor fitting due to the excessive noise in local regions of the input space will then be reflected in large error bars. This is perfectly reasonable from a scientific point of view, but the human tendency is to interpret trends and to neglect the fact that large error bars make it impossible to define trends.
To avoid this perception difficulty, an alternative *constrained* neural network model was created where the network was not allowed to achieve a fit better than 0.15 noise in the normalised output.
To distinguish the two types of models, we shall call the model where σ_v has been fixed the "constrained model", whereas the one where the fitting is allowed to proceed naturally is called "unconstrained model".
The comparisons between the predicted and measured values are presented in the Appendix.

4. Result & Discussion

The neural network models were created using 34 sets of experimental data, each containing three inputs: the welding speed, arc current and laser-power. Each model had one output, which could be the penetration depth, the weld area, the top-width, the bottom-width or height.
Figs. 1~15 show the output (penetration depth, bottom-width, top-width, height, area) as a function of the welding speed for three different values of laser power (1050 W, 1300 W, 1480 W) for a fixed arc current of 35 A.
In the plots discussed below, comparisons will in each case be made between the results from the unconstrained and constrained models; the figures marked (a) are in all cases for the unconstrained model and those marked (b) are from the constrained model
Figs. 1~3 show corresponding plots of the penetration depth as a function of the

welding speed, and laser power. It is evident from Figs. 1~3a that when the importance of the error bars is neglected, the unconstrained model shows unphysical trends in which the penetration increases with the welding speed. The energy transferred during welding decreases as the welding speed increases, so such a trend does not make sense. Note, however, that the Bayesian method works well in that it indicates large uncertainties showing that it is not in fact sensible to deduce the trend shown in Fig. 1a from the data.

By contrast, the corresponding graphs for the constrained model (Figs. 1~3b) show the expected behaviour; it follows that the constrained model can be considered to be a better even though the single experimental point could be perceived to be badly predicted (although within the predicted uncertainty). There is less of a danger of misleading untrained personnel with the constrained model.

When modelling the weld bead area, both kinds of model give reasonable trends, i.e., the amount of material melted decreases as the heat input per unit length decreases (in other words, as the welding speed increases). This is because the weld bead area is a better behaved parameter; Fig. A2 shows a contour plot of the area – it is seen that there is not much noise. Similarly, the predictions of the top width are similar for the two kinds of model; however, the unconstrained model is less certain in its extrapolations because the fitting functions are much more complex. This can be seen from Table. 1 which lists the number of hidden units in each kind of model.

The analysis indicates that the bottom-width is, from an experimental point of view, a badly behaved parameter; it is not therefore surprising that the constrained model show trends which are more reasonable.

Both kinds of model indicate that the reinforcement height should not vary significantly as a function of the weld speed. The experimental data show that the mean and standard deviations of the penetration depth are 1.19±0.45, whereas the corresponding values for the reinforcement height are 0.045±0.02. It is quite possible therefore that many of the measured variations in the reinforcement height are essentially noise. This is proved by examining the values of σ_ν for the unconstrained model; these values are found to be 0.0224, 0.0650, 0.0146, 0.1579, respectively for the area, top width, bottom width and height respectively. The height is perceived to be the most badly behaved experimental parameter! With that interpretation, it is not surprising that all models predict no variation in the height as a function of the welding speed.

One other interesting point to note is that the number of hidden units in the constrained model is smaller than in the unconstrained model. This is because the network heads for simplicity when the data are noisy (Table. 1).

5. CONCLUSIONS

The important conclusions from this comparison of different kinds of neural networks are as follows:

1) It has been shown that it is dangerous to use any neural network model which does not include a treatment of the uncertainty of making predictions in regions of the input space where knowledge is sparse. This is particularly the case when the experimental data are limited (34 examples in this case) or very noisy.

2) For circumstances where the data are noisy, it is useful to constrain the neural network so that the fit achieved is consistent with the noise in the experimental data. This highlights a further point, that it is useful to study the experimental data before proceeding with a neural network analysis.

Reference

1. H .K .D .H Bhadeshia: ISIJ International, **39** (1999),
2. Biffin J , Walduck R.: Plasma Arc Augmented Laser Welding (PALW) Eurojoin 2, Florence (1994)
3. Biffin J , Walduck R.: Plasma Arc Augmented Laser Welding of Aluminum. Laser and Power Beam Processing, (1995),
4. Walduck R , Biffin J.: Plasma Arc Augmented Laser Welding. Welding and Metal Fabrication, **62** (1994),

Depth

Fig 1 a

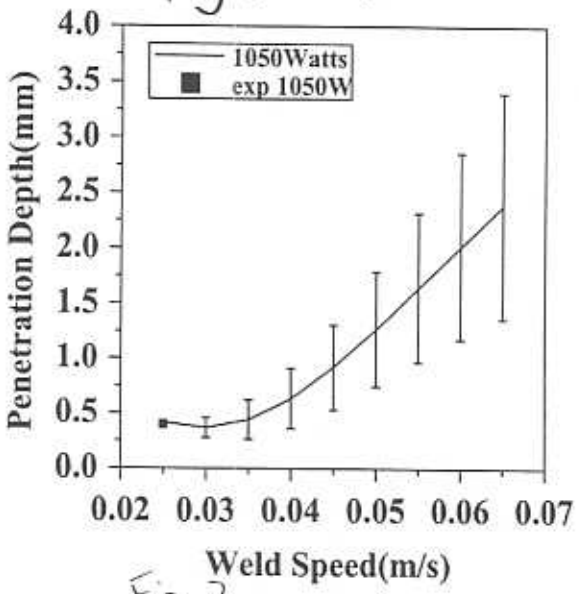

b

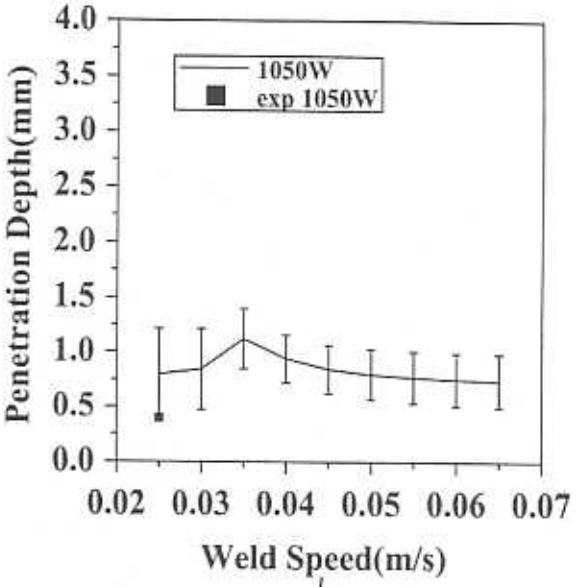

Fig 2 a

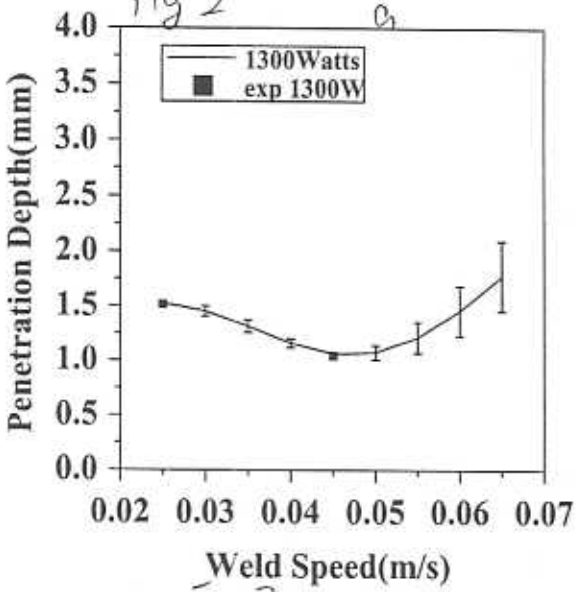

b

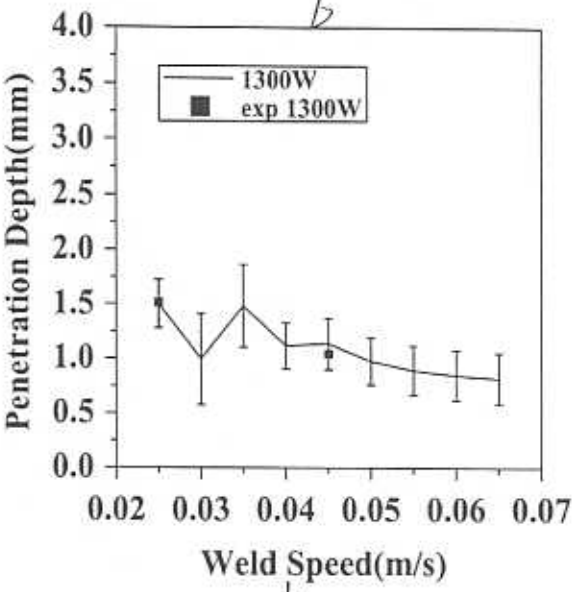

Fig 3 a

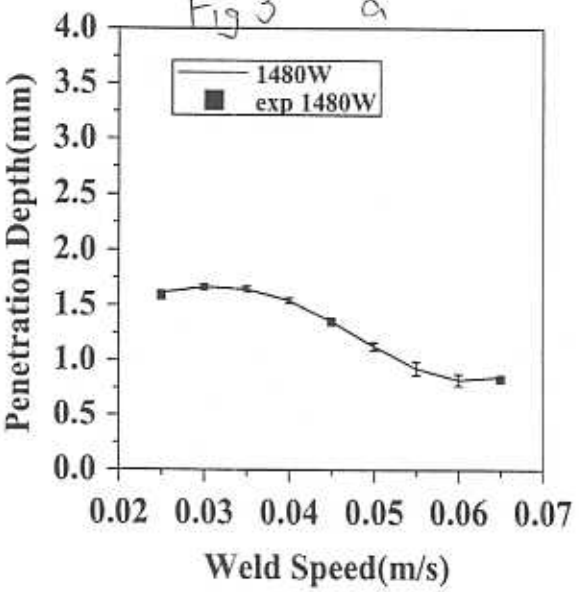

b

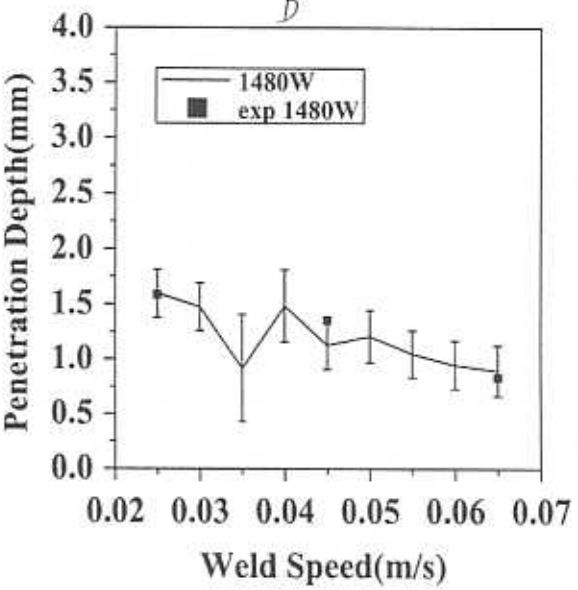

Area

Fig 4 a

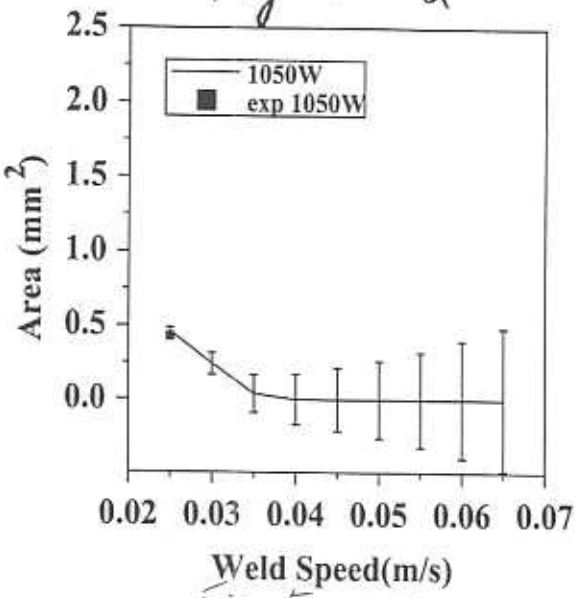

b

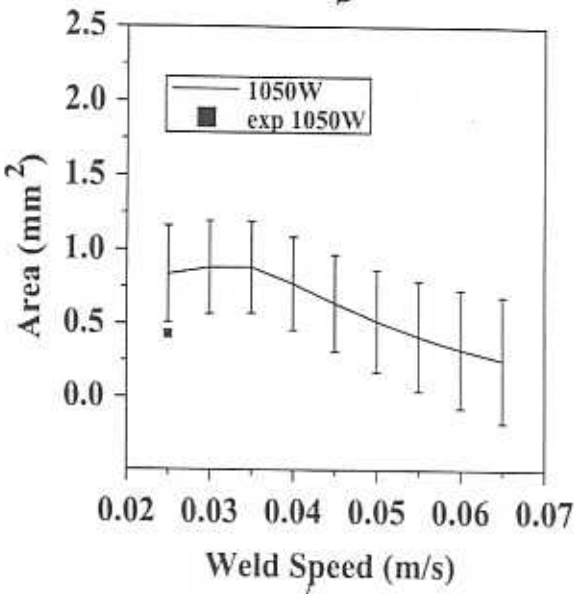

Fig 5 a

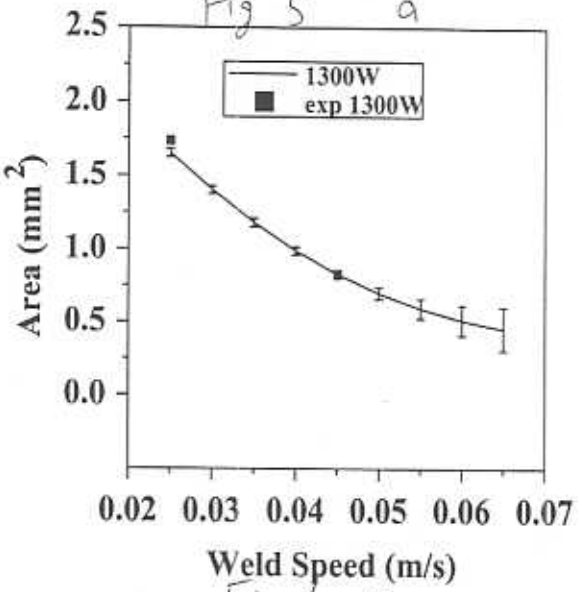

b

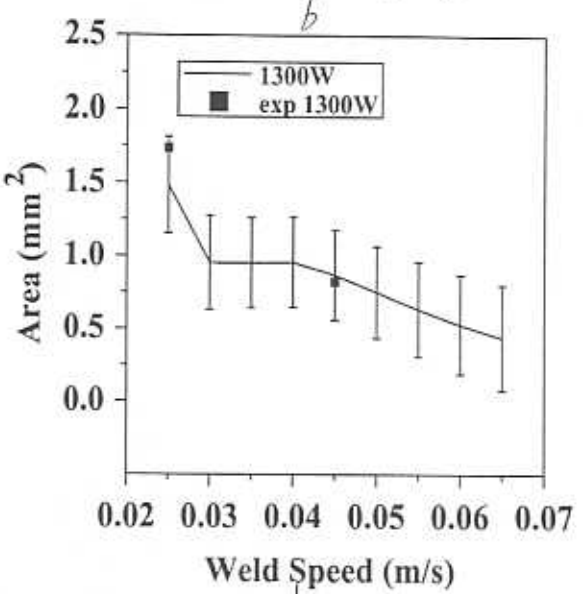

Fig 6 a

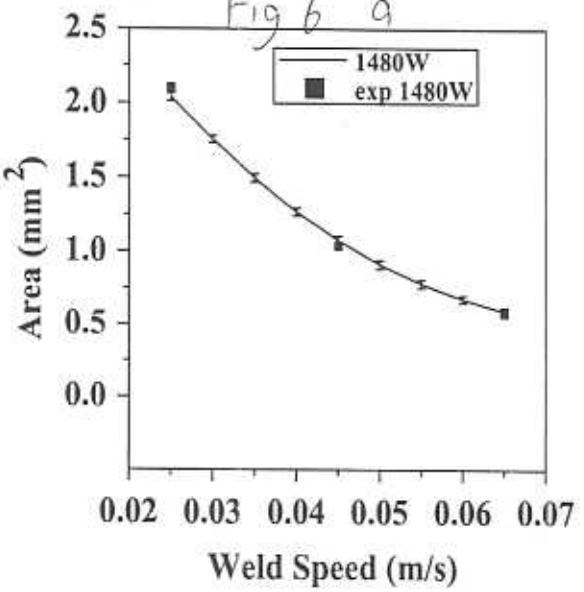

b

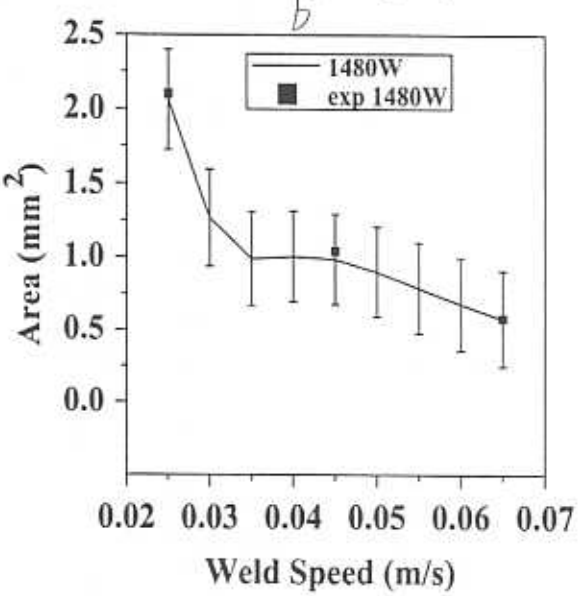

Topwidth

Fig 7a

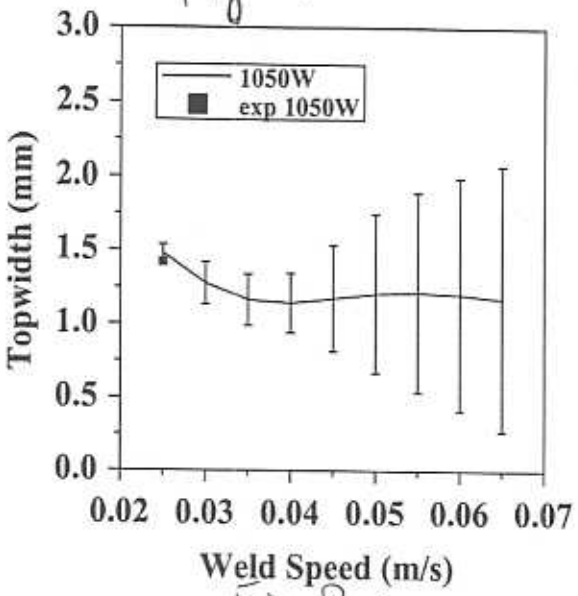

b

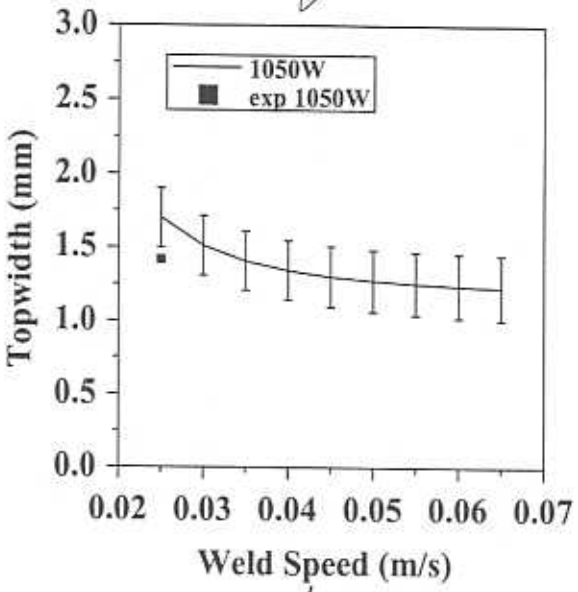

Fig 8 a

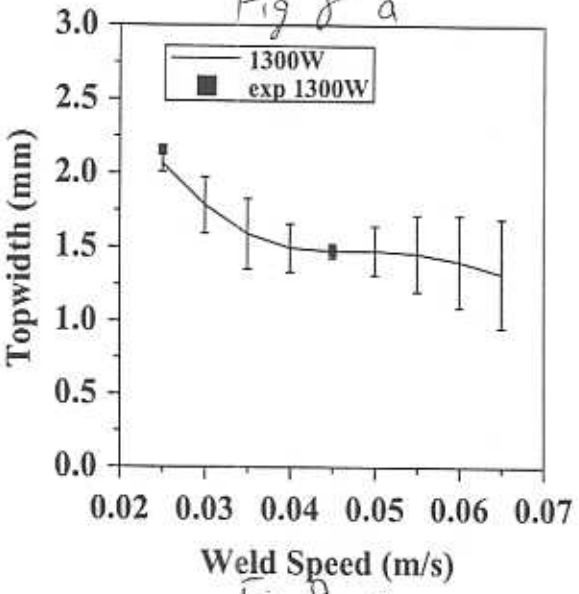

b

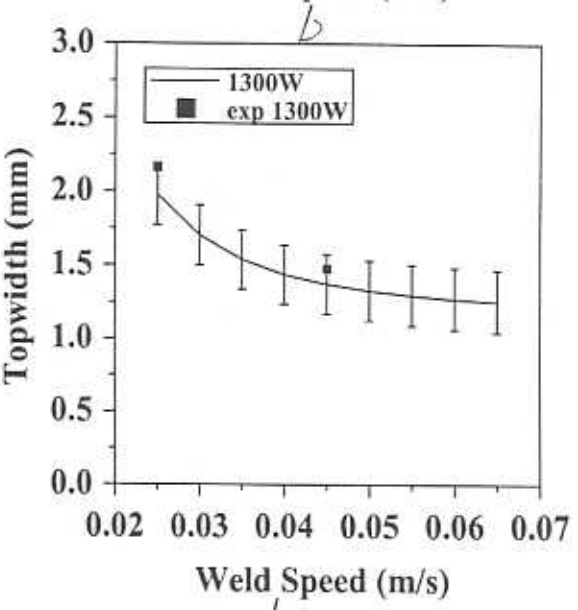

Fig 9 a

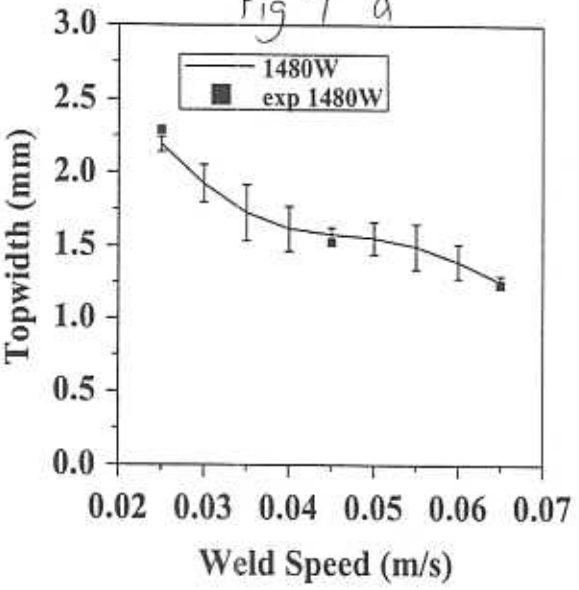

b

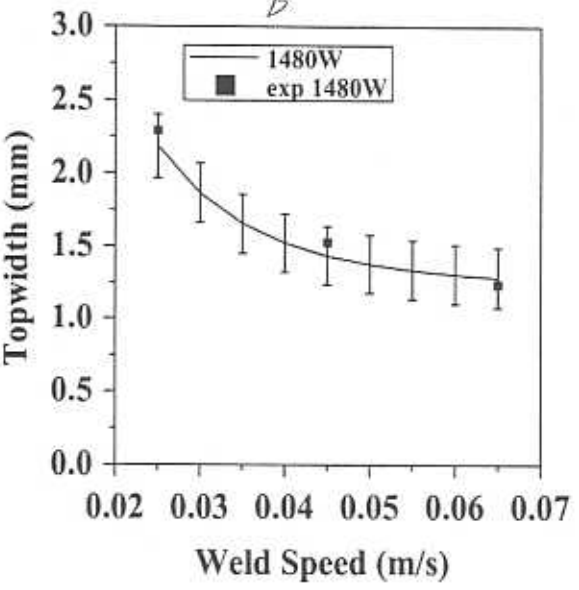

Bottomwidth

Fig 10 a

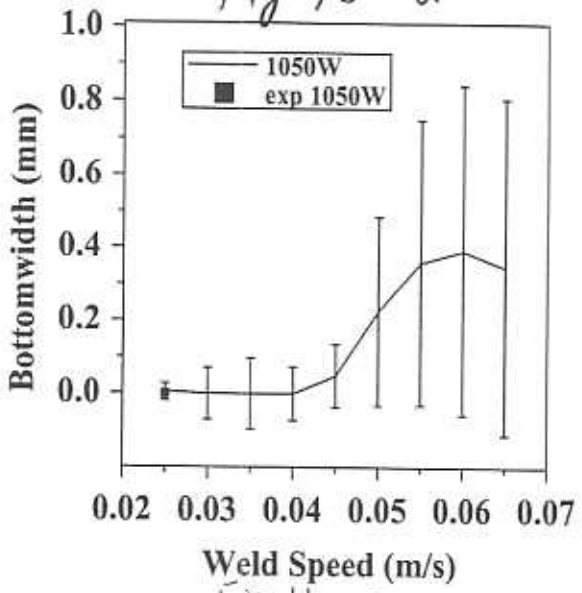

b

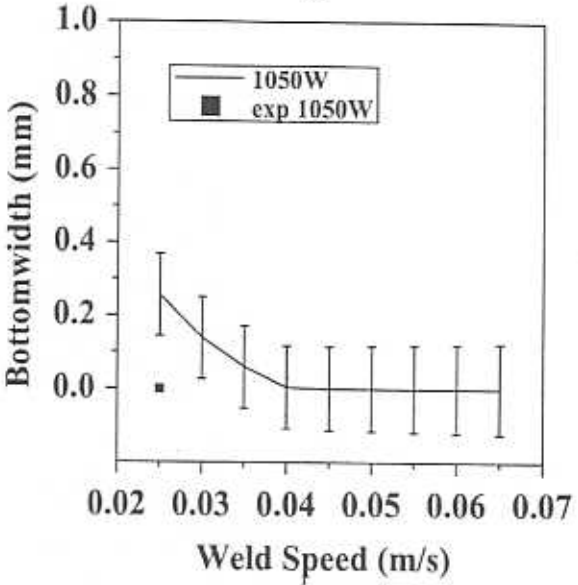

Fig 11 a

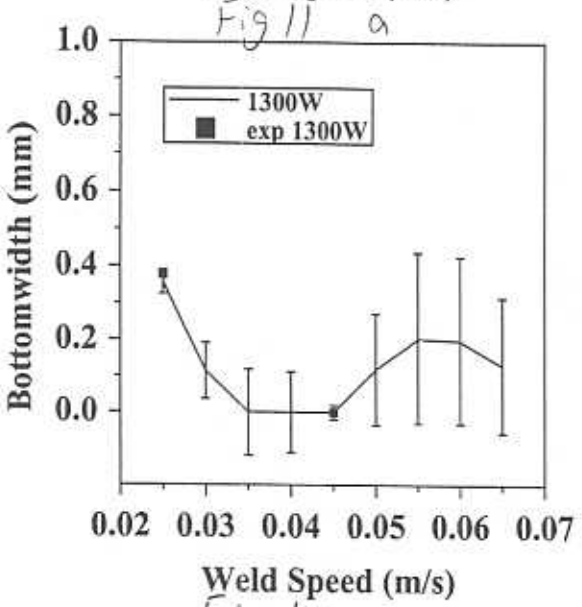

b

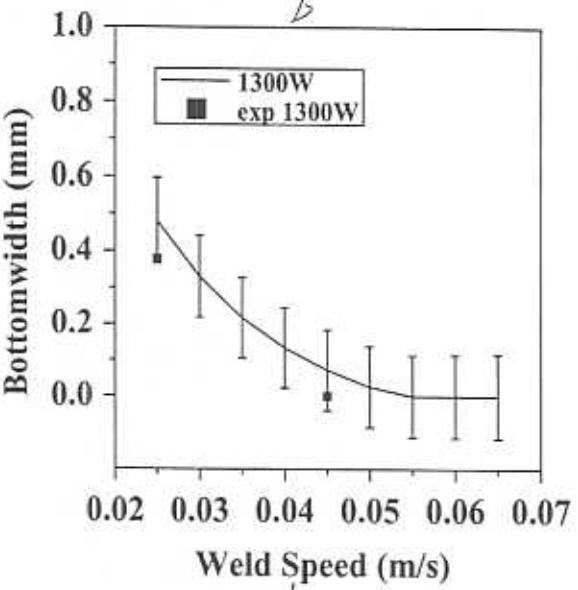

Fig 12 a

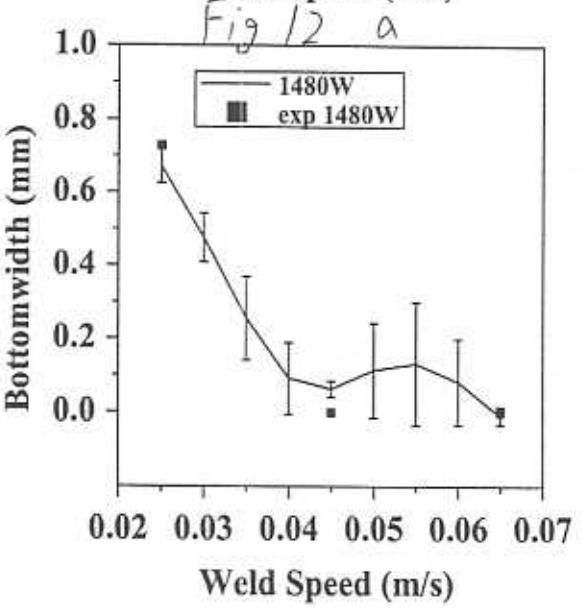

b

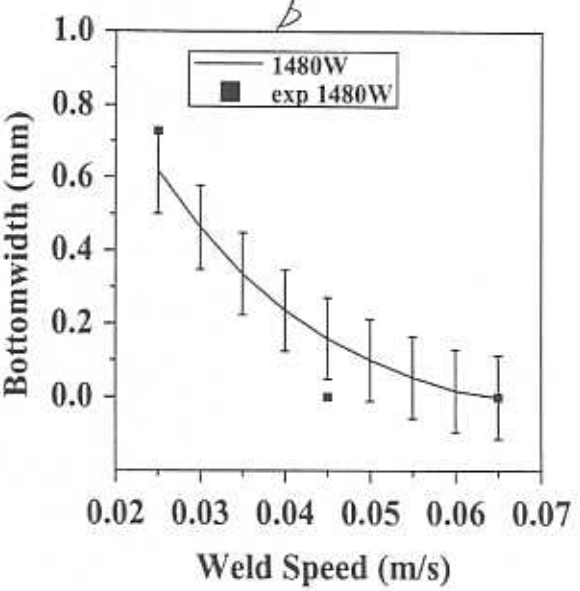

Height

Fig 13 a

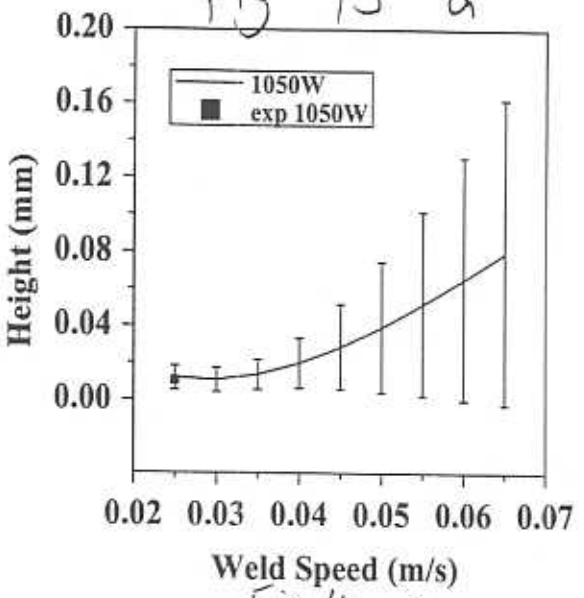

b

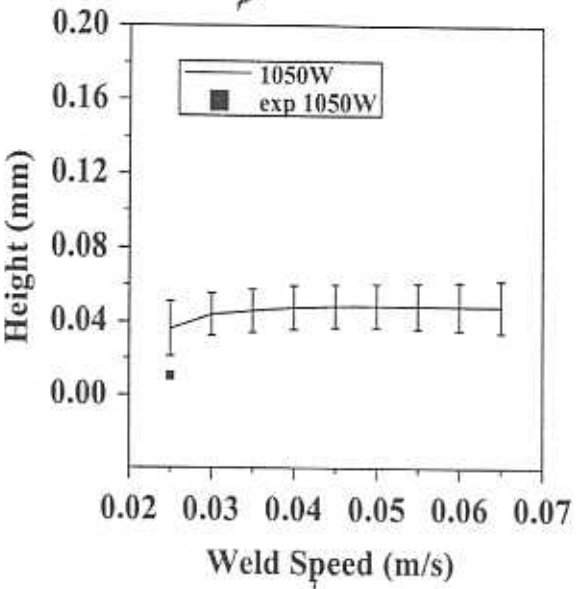

Fig 14 a

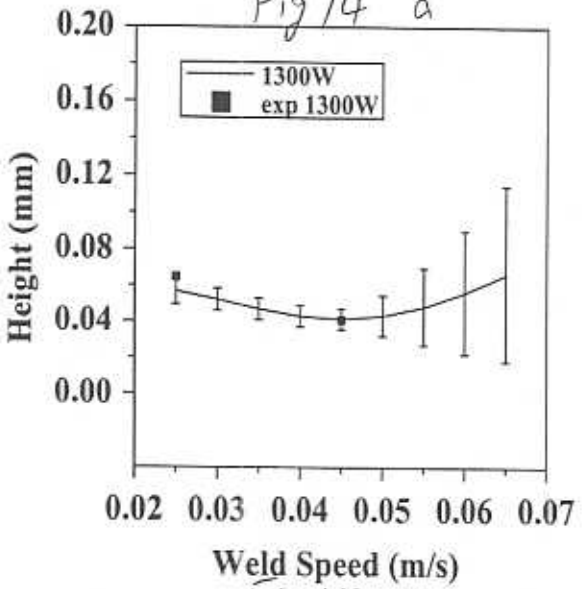

b

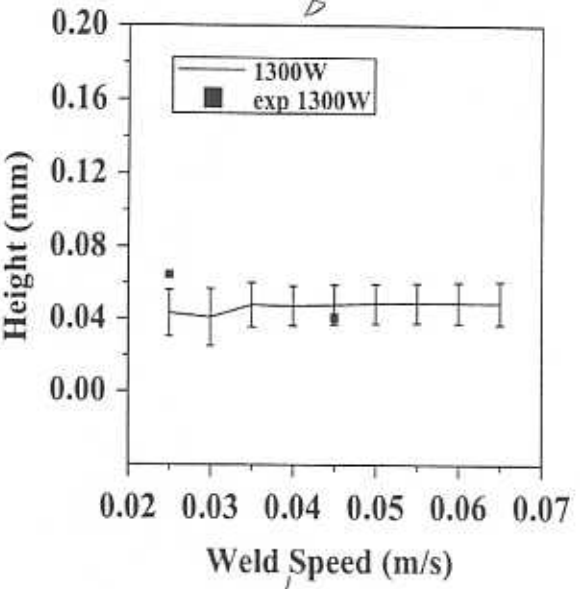

Fig 15 a

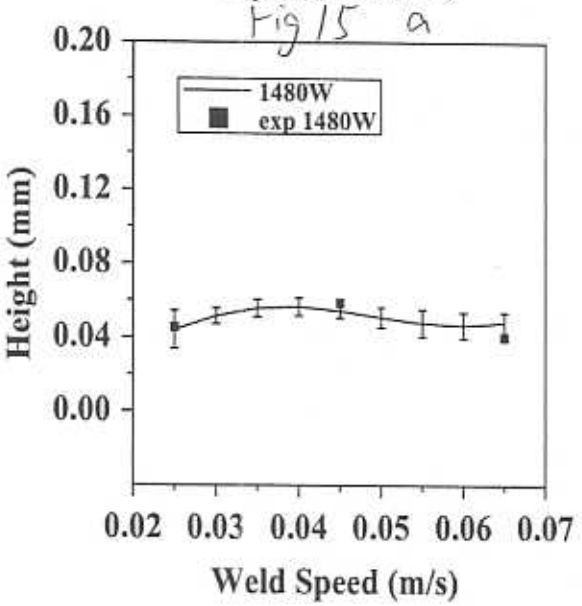

b

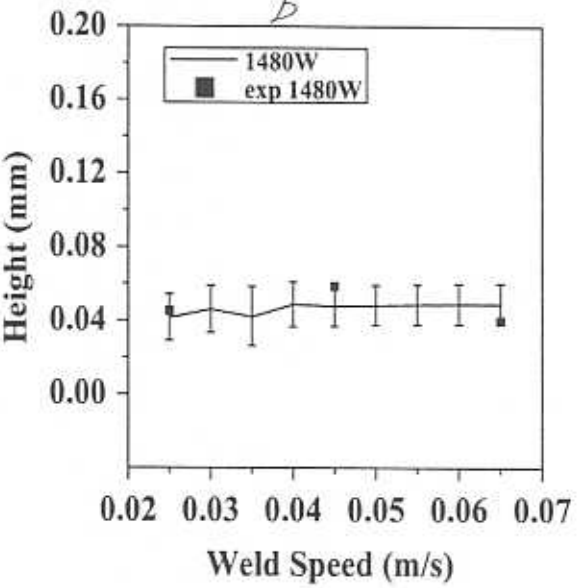

depth

Fig. A1

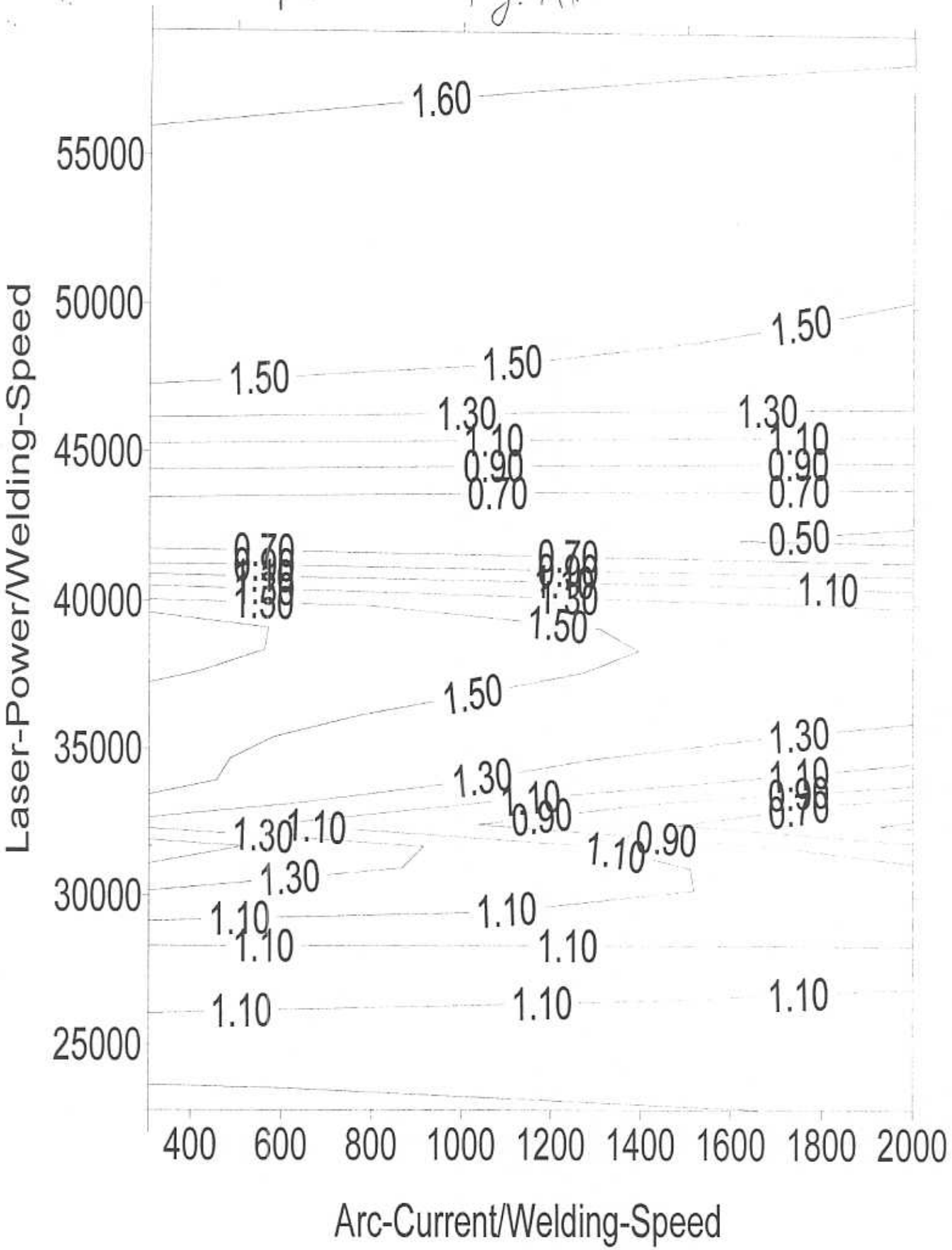
1.60
1.50
1.30
1.10
0.90
0.70
0.50
55000
50000
45000
40000
35000
30000
25000
400
600
800
1000
1200
1400
1600
1800
2000
Laser-Power/Welding-Speed
Arc-Current/Welding-Speed

Area

Fig A2

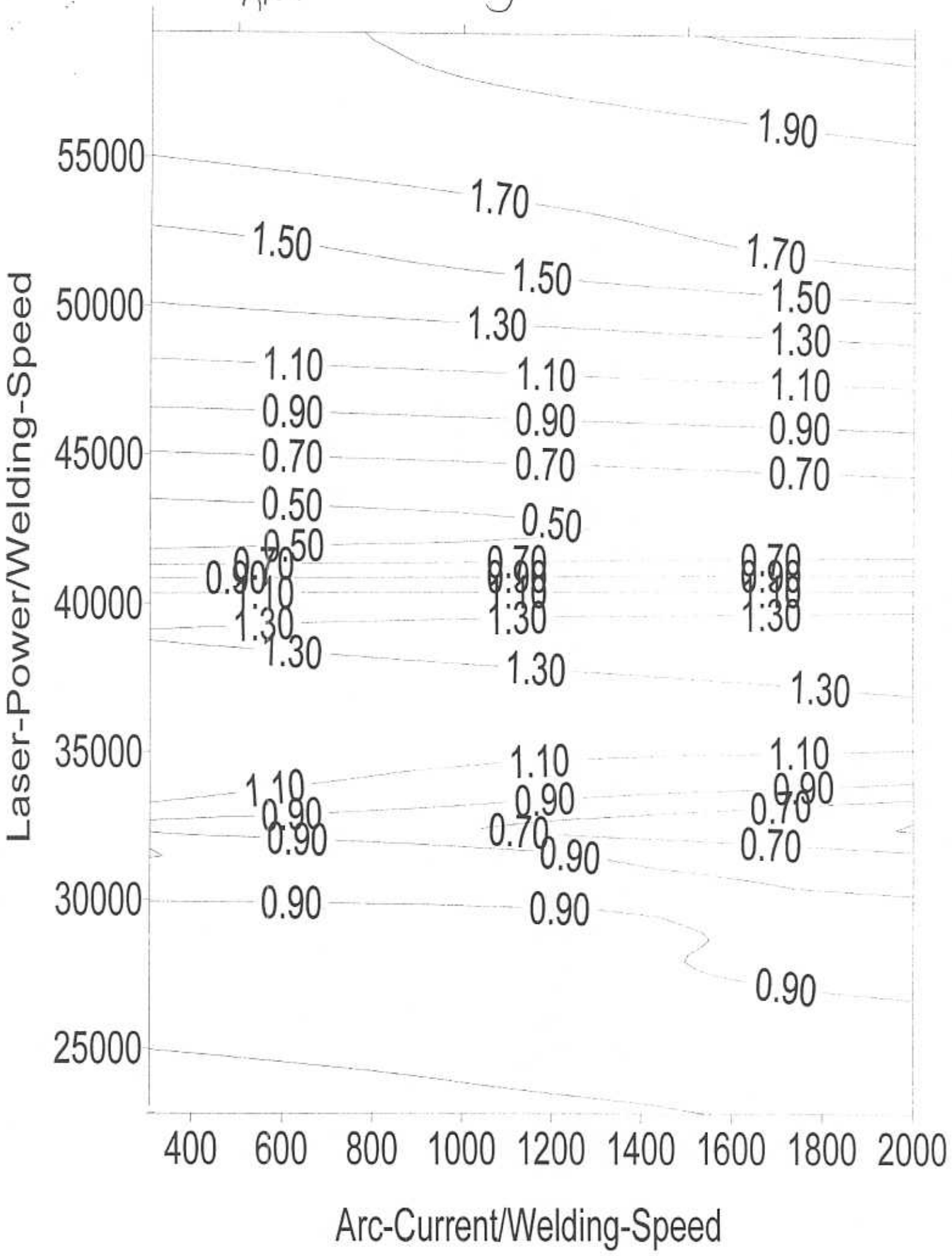
Laser-Power/Welding-Speed
55000
50000
45000
40000
35000
30000
25000
1.90
1.70
1.50
1.30
1.10
0.90
0.70
0.50
400
600
800
1000
1200
1400
1600
1800
2000
Arc-Current/Welding-Speed

Fig. A3a

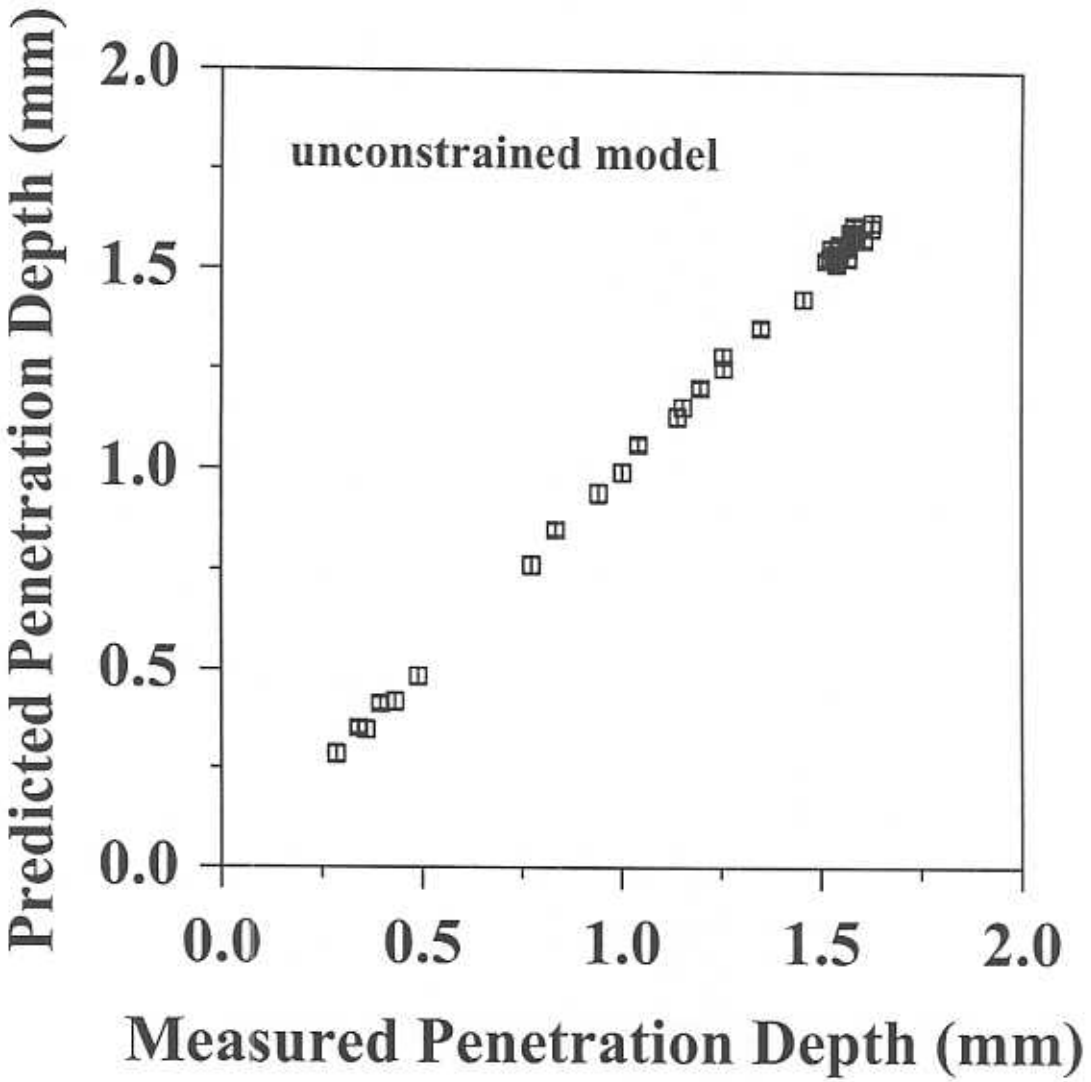
unconstrained model
Predicted Penetration Depth (mm)
Measured Penetration Depth (mm)
0.0
0.5
1.0
1.5
2.0

Fig. A3b

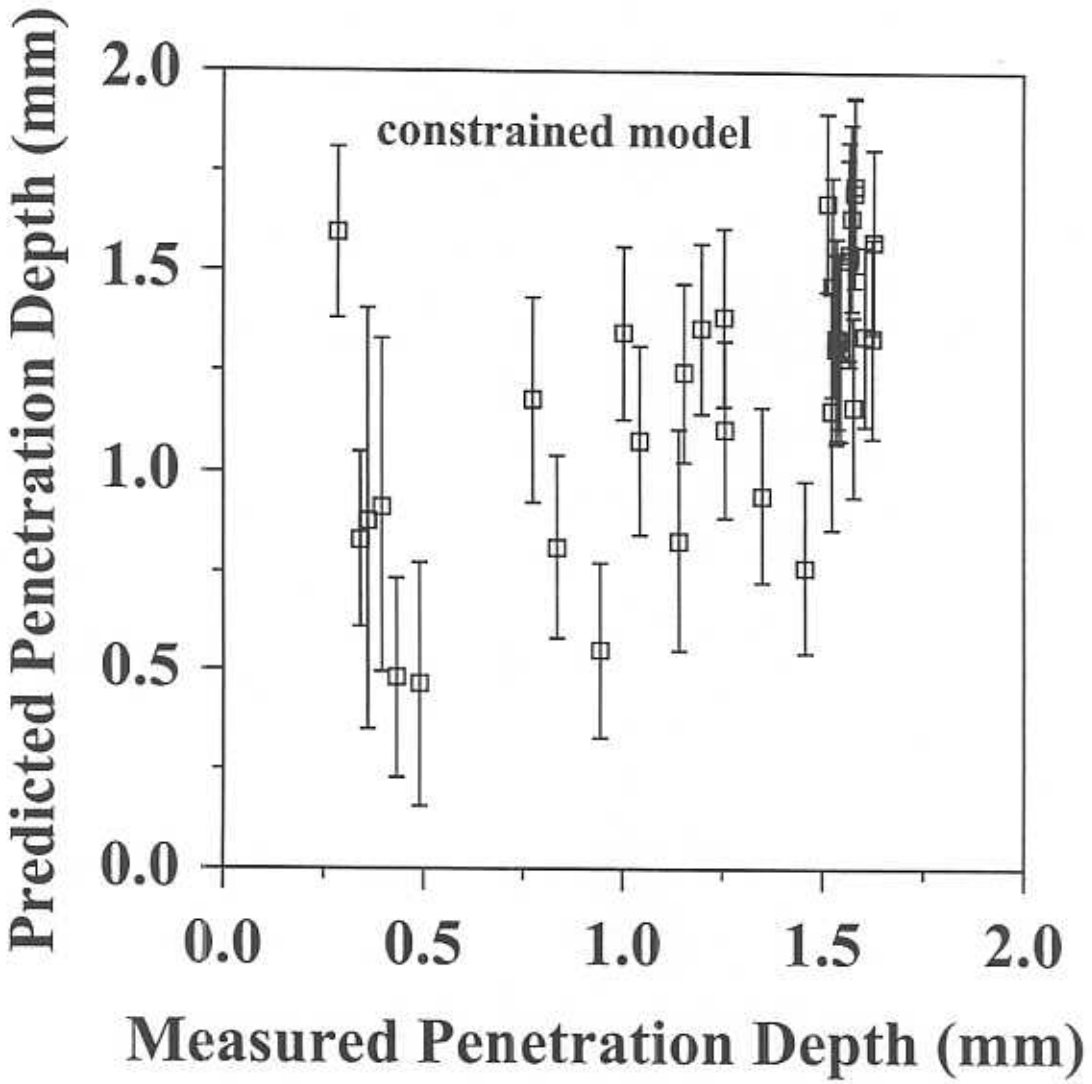
constrained model
Predicted Penetration Depth (mm)
Measured Penetration Depth (mm)
0.0
0.5
1.0
1.5
2.0

A4a

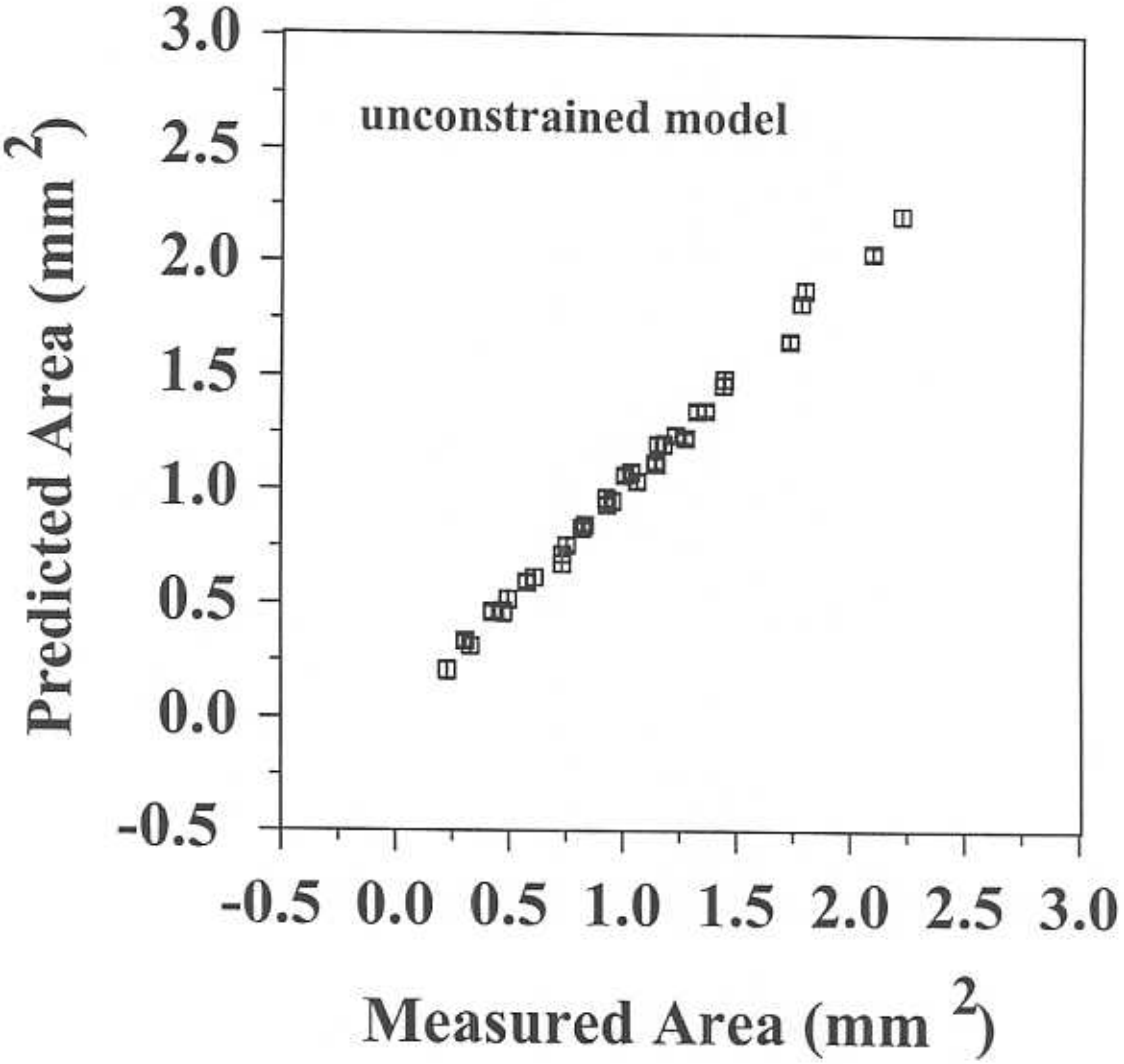
unconstrained model
Predicted Area (mm 2)
Measured Area (mm 2)
3.0
2.5
2.0
1.5
1.0
0.5
0.0
-0.5
-0.5 0.0 0.5 1.0 1.5 2.0 2.5 3.0

A4b

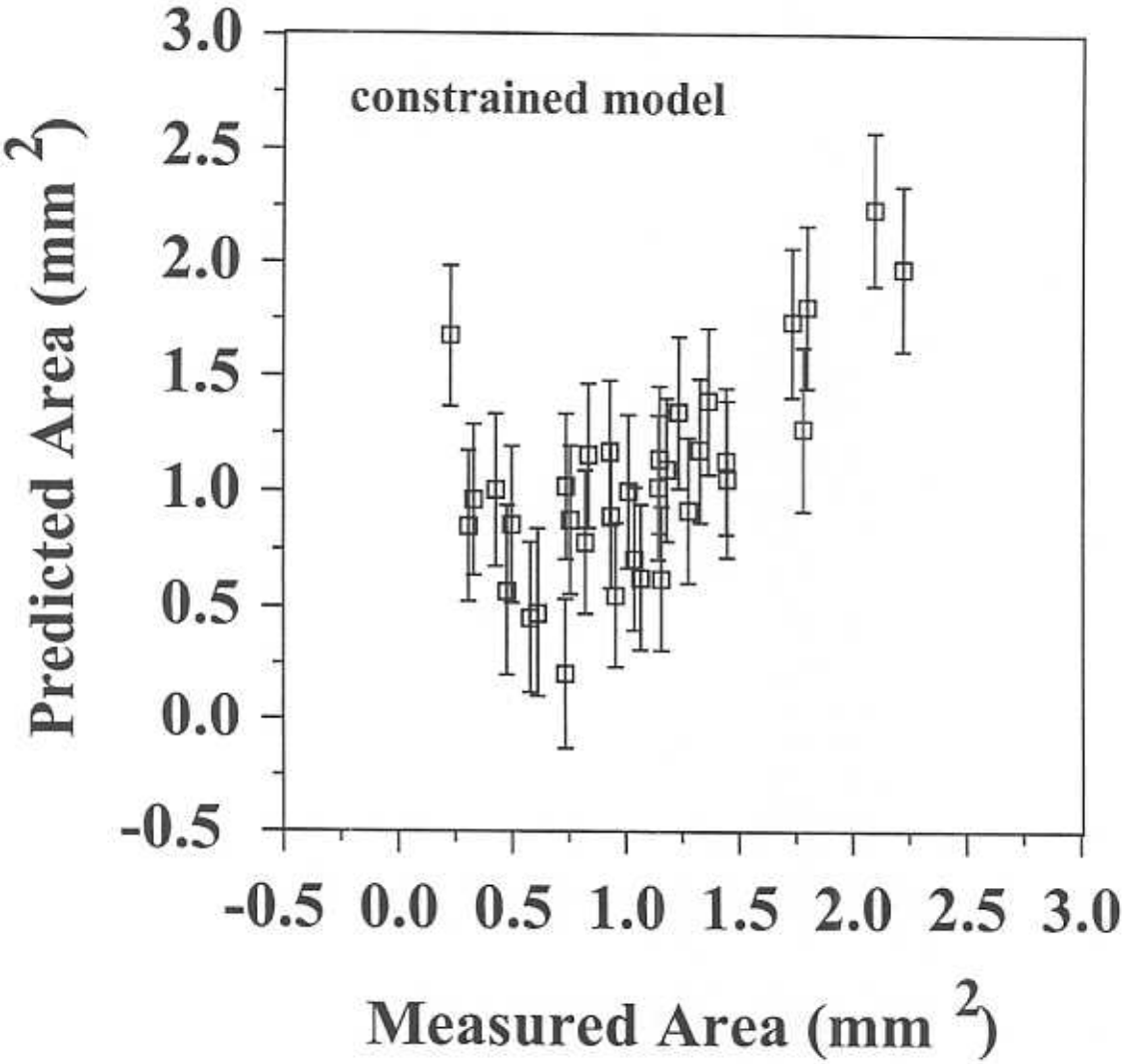
constrained model
Predicted Area (mm 2)
Measured Area (mm 2)
3.0
2.5
2.0
1.5
1.0
0.5
0.0
-0.5
-0.5 0.0 0.5 1.0 1.5 2.0 2.5 3.0

A5a

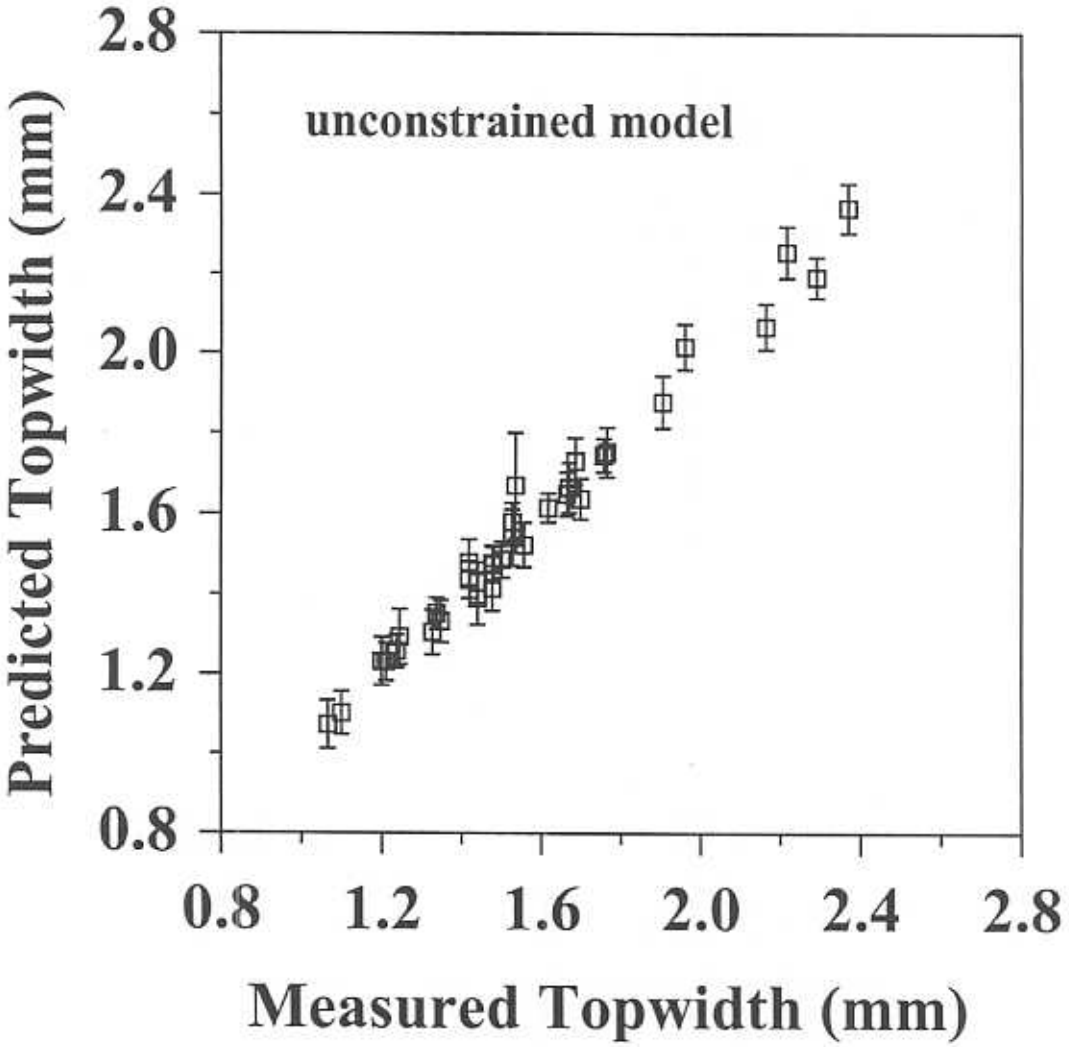
unconstrained model
Predicted Topwidth (mm)
Measured Topwidth (mm)
0.8
1.2
1.6
2.0
2.4
2.8

A 5b

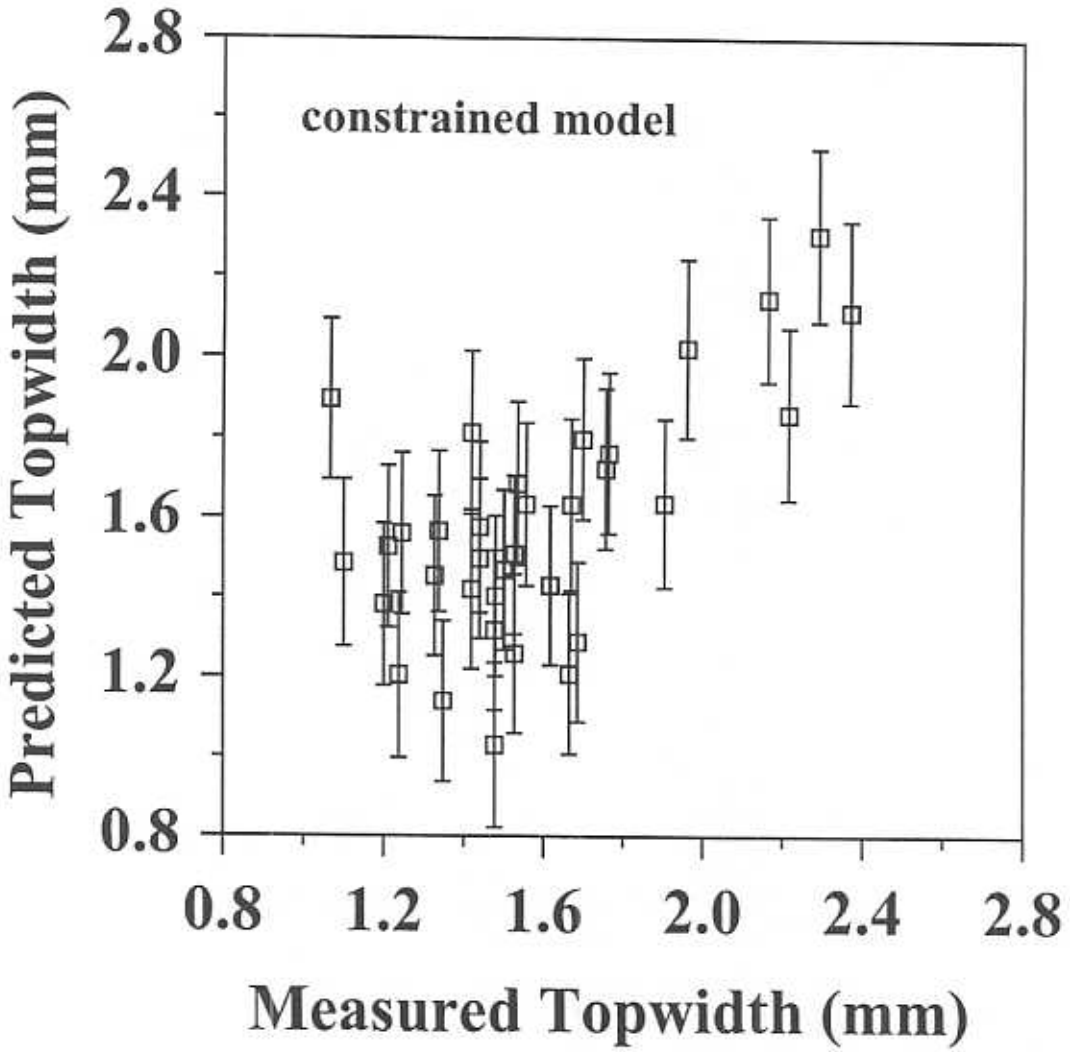
constrained model
Predicted Topwidth (mm)
Measured Topwidth (mm)
0.8
1.2
1.6
2.0
2.4
2.8

A6a

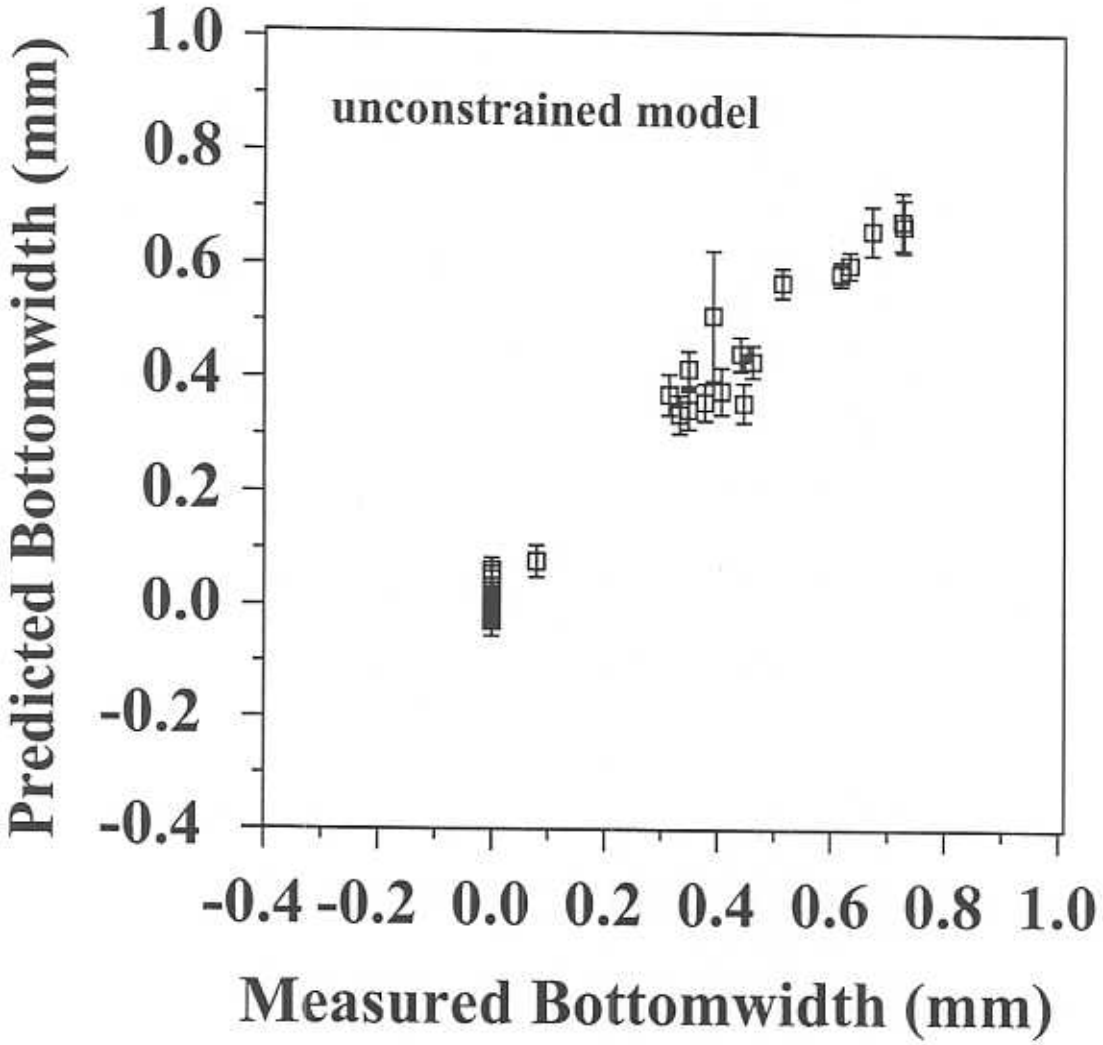
unconstrained model
Predicted Bottomwidth (mm)
1.0
0.8
0.6
0.4
0.2
0.0
-0.2
-0.4
-0.4 -0.2 0.0 0.2 0.4 0.6 0.8 1.0
Measured Bottomwidth (mm)

A66

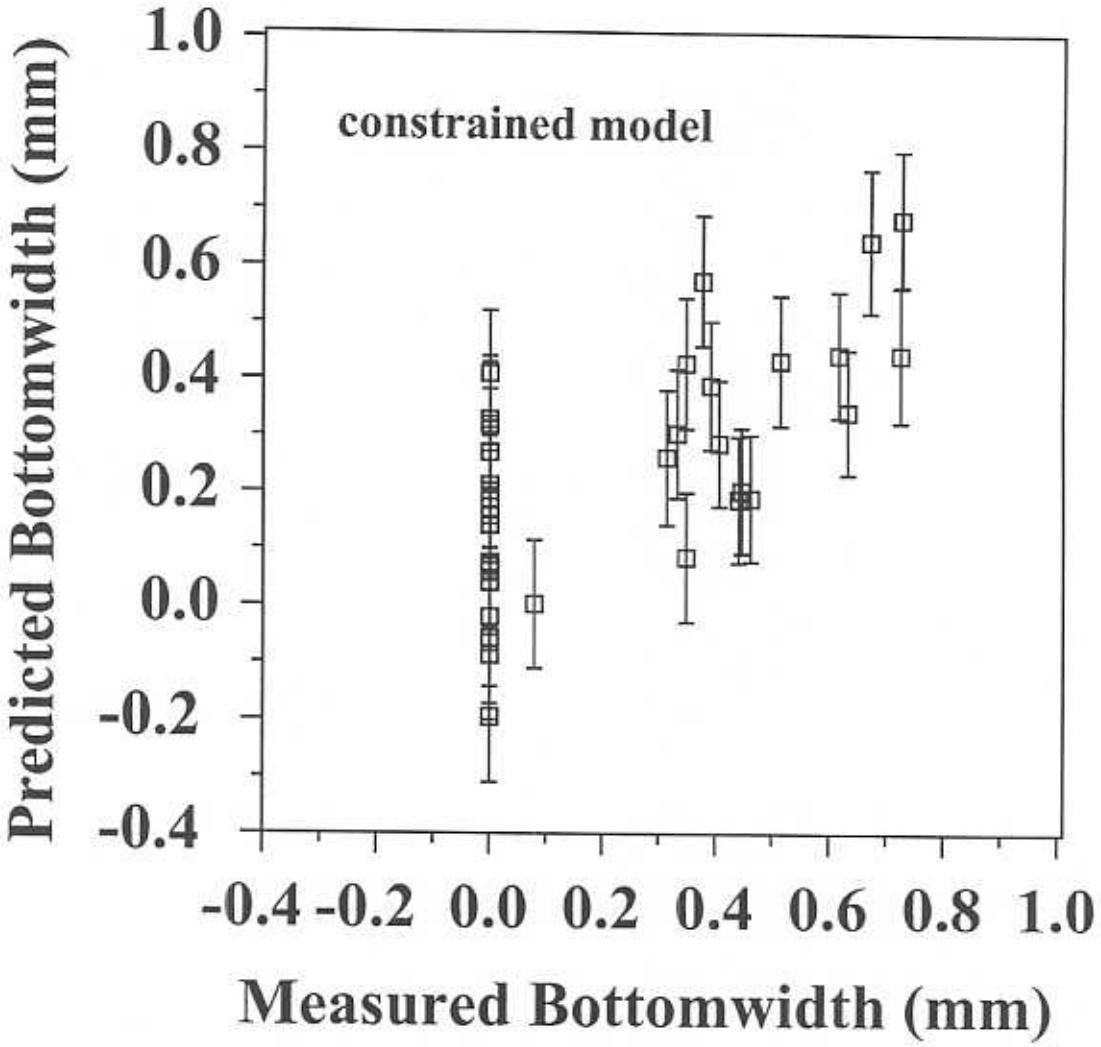
constrained model
Predicted Bottomwidth (mm)
1.0
0.8
0.6
0.4
0.2
0.0
-0.2
-0.4
-0.4 -0.2 0.0 0.2 0.4 0.6 0.8 1.0
Measured Bottomwidth (mm)

A7a

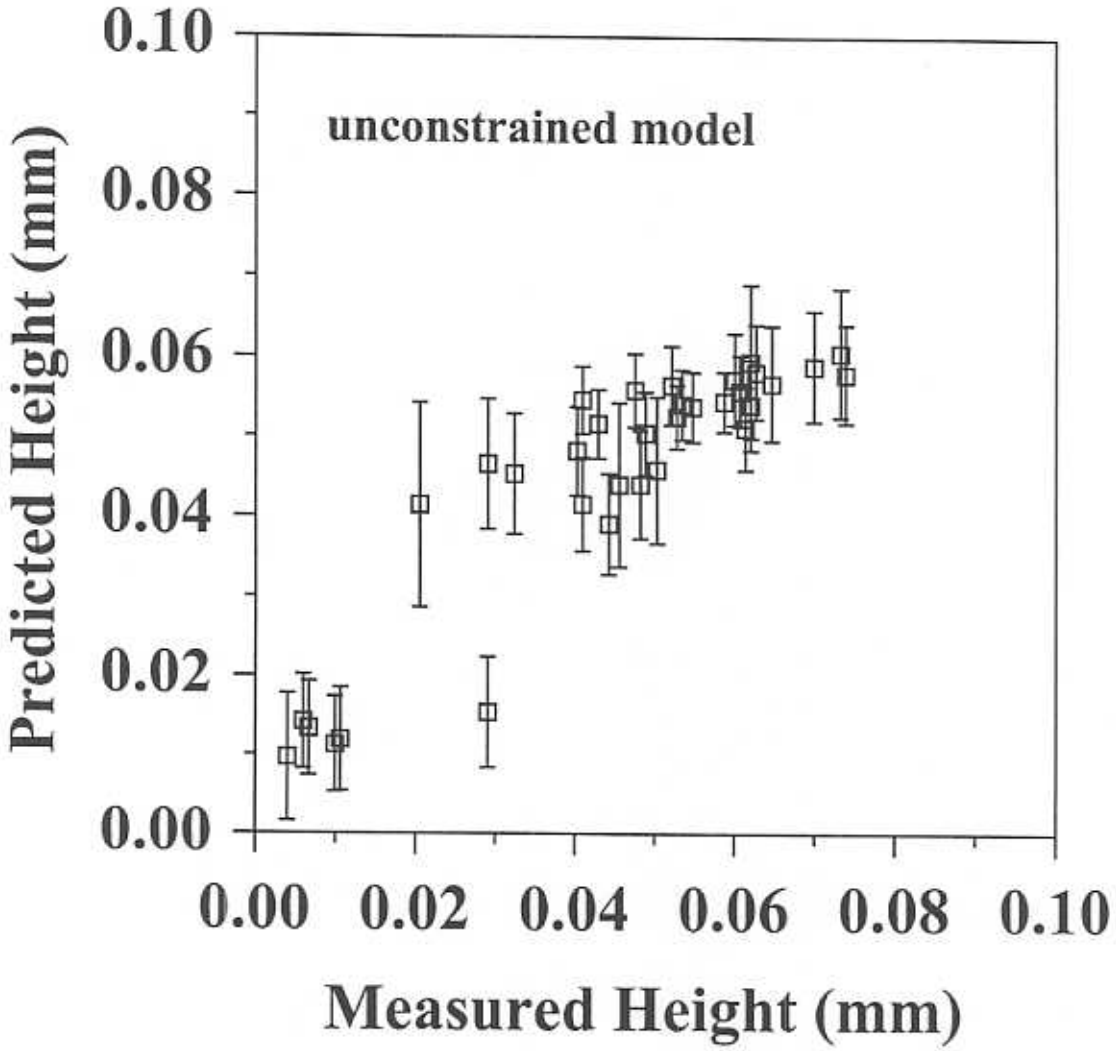
unconstrained model
Predicted Height (mm)
Measured Height (mm)
0.00
0.02
0.04
0.06
0.08
0.10

A7b

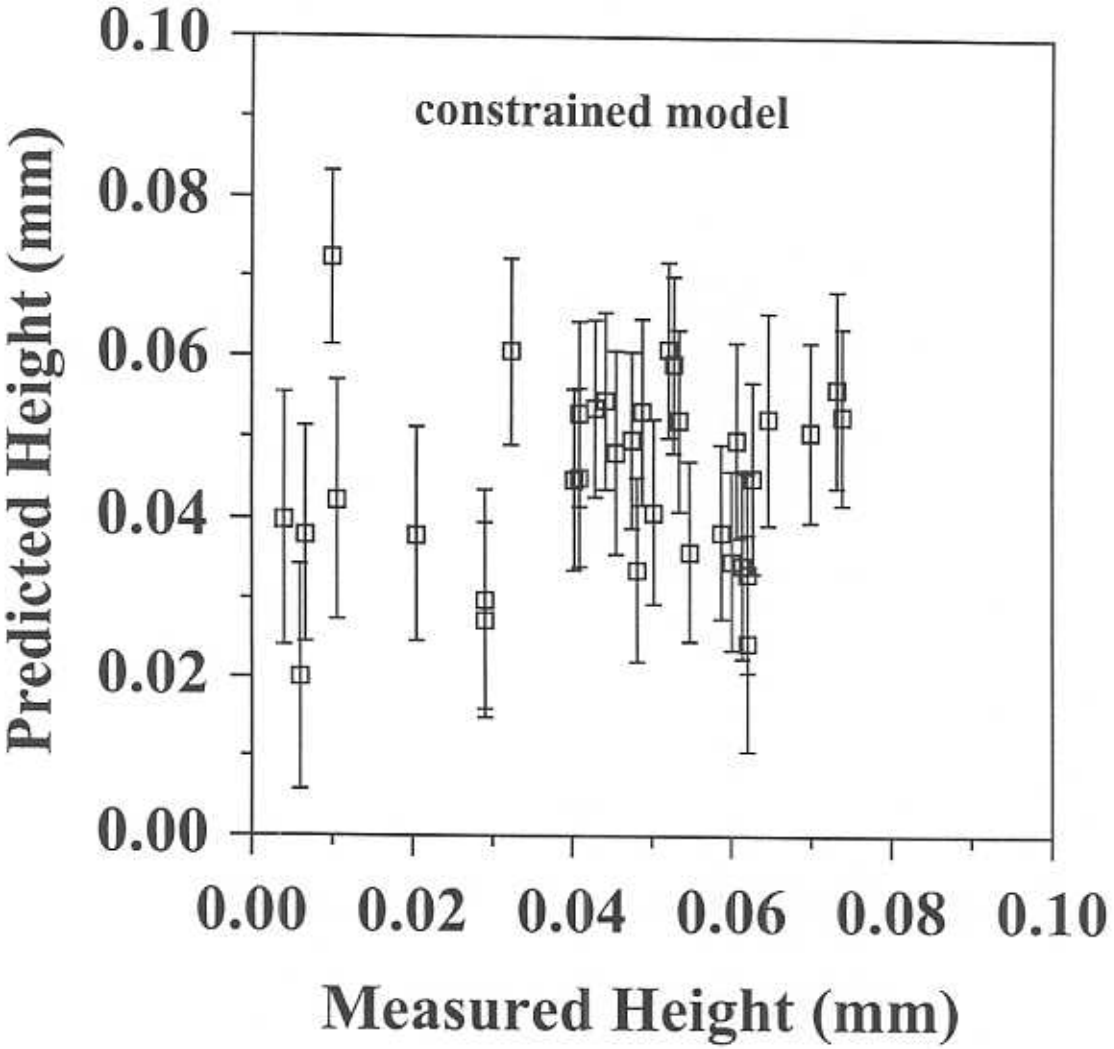
constrained model
Predicted Height (mm)
Measured Height (mm)
0.00
0.02
0.04
0.06
0.08
0.10

Table. 1

	Penetration Depth	Height	Bottom-width	Top-width	Area
Value of σv in *unconstrained model*	0.030	0.1579	0.0146	0.065	0.0224
Value of σv in constrained model	0.150	0.150	0.150	0.150	0.150
Number of Hidden Unit in *unconstrained model*	17	19	3	15	3
Number of Hidden Unit in constrained model	3	10	2	12	18

Penetration depth

Fig1. a: Penetration depth as a function of welding speed with fixed laser power of 1050W and arc current of 35A, which is calculated with the unconstrained model.

Fig1. b: Penetration depth as a function of welding speed with fixed laser power of 1050W and arc current of 35A, which is calculated with the constrained model. The perceived noise level was fixed to 0.15.

Fig2. a: Penetration depth as a function of welding speed with fixed laser power of 1300W and arc current of 35A, which is calculated with the unconstrained model.

Fig2. b: Penetration depth as a function of welding speed with fixed laser power of 1300W and arc current of 35A, which is calculated with the constrained model. The perceived noise level was fixed to 0.15.

Fig3. a: Penetration depth as a function of welding speed with fixed laser power of 1480W and arc current of 35A, which is calculated with the unconstrained model.

Fig3. b: Penetration depth as a function of welding speed with fixed laser power of 1480W and arc current of 35A, which is calculated with the constrained model. The perceived noise level was fixed to 0.15.

Area

Fig4. a: Area as a function of welding speed with fixed laser power of 1050W and arc current of 35A, which is calculated with the unconstrained model.

Fig4. b: Area as a function of welding speed with fixed laser power of 1050W and arc current of 35A, which is calculated with the constrained model. The perceived noise level was fixed to 0.15.

Fig5. a: Area as a function of welding speed with fixed laser power of 1300W and arc current of 35A, which is calculated with the unconstrained model.

Fig5. b: Area as a function of welding speed with fixed laser power of 1300W and arc current of 35A, which is calculated with the constrained model. The perceived noise level was fixed to 0.15.

Fig6. a: Area as a function of welding speed with fixed laser power of 1480W and arc current of 35A, which is calculated with the unconstrained model.

Fig6. b: Area as a function of welding speed with fixed laser power of 1480W and arc current of 35A, which is calculated with the constrained model. The perceived noise level was fixed to 0.15.

Top-width

Fig7. a: Top-width as a function of welding speed with fixed laser power of 1050W and arc current of 35A, which is calculated with the unconstrained model.

Fig7. b: Top-width as a function of welding speed with fixed laser power of 1050W and arc current of 35A, which is calculated with the constrained model. The perceived noise level was fixed to 0.15.

Fig8. a: Top-width as a function of welding speed with fixed laser power of 1300W and arc

current of 35A, which is calculated with the unconstrained model.

Fig8. b: Top-width as a function of welding speed with fixed laser power of 1300W and arc current of 35A, which is calculated with the constrained model. The perceived noise level was fixed to 0.15.

Fig9. a: Top-width as a function of welding speed with fixed laser power of 1480W and arc current of 35A, which is calculated with the unconstrained model.

Fig9. b: Top-width as a function of welding speed with fixed laser power of 1480W and arc current of 35A, which is calculated with the constrained model. The perceived noise level was fixed to 0.15.

Bottom-width

Fig10. a: Bottom-width as a function of welding speed with fixed laser power of 1050W and arc current of 35A, which is calculated with the unconstrained model.

Fig10. b: Bottom-width as a function of welding speed with fixed laser power of 1050W and arc current of 35A, which is calculated with the constrained model. The perceived noise level was fixed to 0.15.

Fig11. a: Bottom-width as a function of welding speed with fixed laser power of 1300W and arc current of 35A, which is calculated with the unconstrained model.

Fig11. b: Bottom-width as a function of welding speed with fixed laser power of 1300W and arc current of 35A, which is calculated with the constrained model. The perceived noise level was fixed to 0.15.

Fig12. a: Bottom-width as a function of welding speed with fixed laser power of 1480W and arc current of 35A, which is calculated with the unconstrained model.

Fig12. b: Bottom-width as a function of welding speed with fixed laser power of 1480W and arc current of 35A, which is calculated with the constrained model. The perceived noise level was fixed to 0.15.

Height

Fig13. a: Height as a function of welding speed with fixed laser power of 1050W and arc current of 35A, which is calculated with the unconstrained model.

Fig13. b: Height as a function of welding speed with fixed laser power of 1050W and arc current of 35A, which is calculated with the constrained model. The perceived noise level was fixed to 0.15.

Fig14. a: Height as a function of welding speed with fixed laser power of 1300W and arc current of 35A, which is calculated with the unconstrained model.

Fig14. b: Height as a function of welding speed with fixed laser power of 1300W and arc current of 35A, which is calculated with the constrained model. The perceived noise level was fixed to 0.15.

Fig15. a: Height as a function of welding speed with fixed laser power of 1480W and arc current of 35A, which is calculated with the unconstrained model.

Fig15. b: Height as a function of welding speed with fixed laser power of 1480W and arc current of 35A, which is calculated with the constrained model. The perceived noise level was fixed to 0.15.

Table. 1: Value of σ_V and number of Hidden Units in the unconstrained and constrained model for 5 parameter.

Appendix

Fig. A1: Contour plot of penetration depth as a function of Arc-Current/Welding-Speed and Laser-power/Welding-Speed.

Fig. A2: Contour plot of area as a function of Arc-Current/Welding-Speed and Laser-power/Welding-Speed.

Fig. A3a: Predicted *versus* measured penetration depth in unconstrained model.

Fig. A3b: Predicted *versus* measured penetration depth in constrained model.

Fig. A4a: Predicted *versus* measured area in unconstrained model.

Fig. A4b: Predicted *versus* measured area in constrained model.

Fig. A5a: Predicted *versus* measured top-width in unconstrained model.

Fig. A5b: Predicted *versus* measured top-width in constrained model.

Fig. A6a: Predicted *versus* measured bottom-width in unconstrained model.

Fig. A6b: Predicted *versus* measured bottom-width in constrained model.

Fig. A7a: Predicted *versus* measured height in unconstrained model.

Fig. A7b: Predicted *versus* measured height in constrained model.